Наносистеми, наноматеріали, нанотехнології
Nanosistemi, Nanomateriali, Nanotehnologii
2026, т. 24, № 2, сс. 419–430
https://doi.org/10.15407/nnn.24.02.0419

PACS numbers: 78.20.Ci, 78.30.Hv, 78.55.Qr, 78.67.Qa, 78.70.En, 81.20.Fw, 82.33.Ln

Studying the Optical Features of Silica Xerogel Doped with Cerium (Ce) for Gamma Ray Detection

Abdul-Jabbar Abbas Oudh[1], Mohammed Jawad H. Kadhim[2], Abdul Kareem Abdul-Hussein[3], and Zainab Al-Khafaji[4,5]

[1]*State Company for Foodstuffs Trading,*
Department of Quality Control,
Ministry of Trade,
Baghdad, Iraq
[2]*Materials Engineering College,*
Department of Polymer Engineering,
University of Babylon,
Hillah Iraq
[3]*University of Information Technology and Communications,*
Al-Nidhal Str.
Baghdad, Iraq
[4]*Department of Civil Engineering,*
Faculty of Engineering and Built Environment,
Universiti Kebangsaan Malaysia,
43600 UKM Bangi, Selangor, Malaysia
[5]*Imam Ja'afar Al-Sadiq University,*
Hay Alqahira,
Baghdad, Iraq

Ionic Ce-doped xerogel of silica is synthesized for gamma ray detecting by the sol–gel method and subsequent densification in an inert gas (argon) atmosphere. The optical characteristics may be enhanced by sintering the xerogel in an argon gas, *i.e.*, with a procedure that increases the photoluminescence quantum yield due to a greater concentration of Ce^{+3} ions. A glassy rod is fabricated at elevated temperatures for the specimen, which is later utilized for gamma ray radiation monitoring. The strength of the radioluminescent signal in the Ce-doped rod increases significantly with escalating dosages of gamma rays till it approaches 500 rad, making this material a *via*ble choice for radiation detection utilization in hostile environments.

Йонний ксероґель кремнезему, леґований Церієм, синтезовано для детектування гамма-променів золь–ґель-методом і подальшим ущільненням в атмосфері інертного газу (арґону). Оптичні характеристики мож-

на поліпшити спіканням ксероґеля в арґоні, що підвищує квантовий вихід фотолюмінесценції завдяки більшій концентрації йонів Ce^{3+}. Для зразка за підвищених температур виготовлено склоподібний стрижень, який пізніше використано для моніторинґу гамма-випромінення. Сила радіолюмінесцентного сиґналу у стрижні, леґованому Церієм, значно зростає зі збільшенням доз гамма-променів, поки вона не наблизиться до 500 рад, що робить цей матеріял життєздатним вибором для використання у детектуванні випромінення в аґресивних середовищах.

Key words: xerogel of silica, gamma ray detection by radioluminescent signal.

Ключові слова: ксероґель кремнезему, детектування γ-випромінення радіолюмінесцентним сиґналом.

(Received 6 October, 2024; in revised form, 13 October, 2024)

1. INTRODUCTION

The surveillance and identification of radiation from ions in the environment, whether from inadvertent nuclear incidents or exposure at work, are essential for soldiers and radiation professionals in healthcare and the nuclear sector [1–3]. The significance of radiation monitoring has increased markedly since the 9/11 terrorist attacks in the United States in 2001. While several nuclear equipments exist for environmental radiation monitoring, they are not only costly but also need specialized assistance for operation and maintenance. Furthermore, it is recognized that the nuclear environment poses risks to equipment used for normal operations. A significant problem arises, when temperatures increase during nuclear explosions, causing many forms of monitoring equipment to fail. Nevertheless, it might be impractical to install readily accessible instruments rapidly at several sites during nuclear crises, or to monitor levels of radiation across various geographical regions. Consequently, appropriate radiation monitoring systems must be devised [4, 5].

In radiation, dosimetry is used to measure the energy deposited in a substance or absorbed by a person from radiation sources. Diverse dosimetry systems are used for various applications in industrial and research irradiation facilities, each with distinct needs for dosage assessments [6]. Radioactive safety requirements and concerns for protecting of people from exposure to radiation are governed by specific dosimetry metrology.

Radiation dosimetry is a discipline within the physical science that investigates several techniques for the quantitative assessment of energy deposited in a specific substance by ionizing radiation,

whether by direct or indirect exposure. Dosimetry pertains to the assessment and computation of doses that quantify the energy absorbed by a substance. Dosimetry assessments conducted by subjecting a dosimeter to a radiation source facilitate the evaluation of radiation-induced effects—physical, chemical, and/or biological ones—on irradiated materials [7].

Validation and process control techniques are used to ensure that the intended impact of radiation (physical, biological, and chemical one) is realized and that the process of irradiation is carried out safely. For isotropic radioactive source irradiators, this relationship is established by the dwell duration, position in the source rack, and conveyance speed; for accelerator sources, it is established by the conveyance speed, scanned uniformity, scanning width, beam current, and beam voltage. Therefore, process controls are dependent on this association being established. Inferences about absorbed dosage and dose distribution are derived from measurements performed utilizing an appropriate dosimetry device with a certain degree of precision and accuracy [8].

Limited literature exists about the prospective applying of optical fibres coated with rare earth elements by the sol–gel technique for radiation dosimetry in nuclear plants. Radiation hardness is a common phenomenon in optical fibre, marked by an increase in the visible light absorption within a particular wavelength varying as the radiation that is absorbed dose increases [9]. This study primarily used γ-radiation to irradiate a sol–gel glassy matrix with different probing elements or molecules, with the absorbed radiation amount quantified utilizing luminescent or absorption studies. The fluorescence and absorption assessing techniques are simple and might be modified for portable readout equipment. The development of sol–gel-based radiation-sensitive materials was a primary research focus of our attention [4].

The novelty of this study lies in the development and investigation of ionic Ce-doped xerogel of silica as a novel material for gamma ray detection, produced *via* the sol–gel route and densified under inert argon gas. This approach uniquely enhances the optical properties of the xerogel, particularly, improving the photoluminescence quantum yield due to the increased concentration of Ce^{3+} ions during the sintering process. A key innovation is the production of a glassy rod from the doped xerogel, drawn at high temperatures, which exhibits a significant increase in radioluminescent (RL) signal intensity with increasing gamma ray doses up to 500 rad. This significant RL response demonstrates the material's potential for efficient gamma ray detection, particularly, in harsh environments, where other materials may fail. The study's importance lies in its contribution to the field of radiation detection, offering a promis-

ing new material that combines high sensitivity with durability, which could prove critical in applications requiring precise and reliable radiation monitoring. Nanoporous silica monoliths have been produced utilizing a polymer sol–gel technique, utilizing tetraethylorthosilicate (TEOS) as the precursor. The achieved xerogels have been stabilized at 900°C and submerged in an alcoholic solution with Ce-chloride $CeCl_3 \cdot 7H_2O$. The use of Ce-doped xerogel of silica as a gamma ray detector represents a step forward in developing new detection technologies for challenging environments, such as nuclear power plants, space missions, and medical radiation therapy.

2. EXPERIMENTAL PART

2.1. Specimens' Production and Treatments

The first part of the construction includes the fabrication of a cylindrical rod utilizing the sol–gel technique. This method was chosen due to its ability to produce transparent glass at far lower temperatures, including hundreds of degrees below the necessary temperature of reaction for this process. This study involves the xerogel-of-silica manufacture including Ce-chloride $CeCl_3 \cdot 7H_2O$. The experimental conditions have been modified to enable specimen creation by the sol–gel method at neutral pH. The selected rare-earth element Ce was selected since to its superior luminescence. The produced specimens possess a molar amount of $4 \cdot 10^{-2}$ mol/litre and have undergone densification in an inert gas (argon) [10].

Nanoporous silica monoliths have been produced utilizing a polymer sol–gel technique, utilizing tetraethylorthosilicate (TEOS) as the precursor. The achieved xerogels have been stabilized at 900°C and submerged in an alcoholic solution with Ce-chloride $CeCl_3 \cdot 7H_2O$. The specimens were removed from the doped solution and dried at 50°C for a period to eliminate solvents and retain the Ce component inside the nanopores. The doped matrices were then densified in an inert gas (argon) at the prescribed situations [11].

Xerogels of silica, both non-doped and Ce-doped ones, were produced with the same method for comparative purposes. Four types of specimens of xerogel of silica were developed and designated as SiO_2CeAr and SiO_2Ar. Upon meticulous cutting and polishing, the resultant glasses display no fractures and have exceptional clarity, as detected in Fig. 1.

Finally, irradiation the samples by gamma ray (Cs-137) have energy of 60 keV, activity of 7 mCi, and the 2.5 cm distance between the source and samples with different gamma ray doses of 100, 200, 400, 500, and 2400 rad.

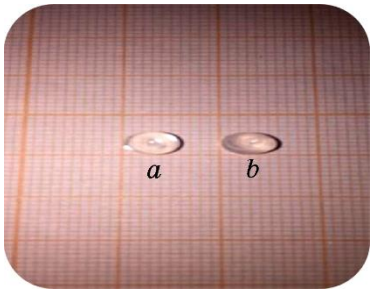

Fig. 1. The images: *a*) SiO_2Ar; *b*) SiO_2CeAr.

TABLE 1. The equipment and apparatus utilized for this research.

Tools	Companies	Originality
Spectrophotometer	EMC-LAB	
pH-meter	Sartorius	
Oven	Memmert	Germany
Analytical Balance	Sartorius	
Scientific furnace	Nabertherm	
	Barnstead International	USA
Stirrer	Stuart	UK
FT-IR-spectrophotometer	SHIMADZU	Japan

2.2. Characterization Methods

The densification of the specimens, which were produced under inert gas (argon), was analyzed with various measuring instruments, involving Fourier transform infrared (FT-IR) spectroscopy, fluorescence spectrophotometry, and spectroscopy UV–visible spectrophotometry, all of which are explained in this work as illustrated in Table 1.

3. RESULTS AND DISCUSSION

3.1. Fourier Transform IR Spectroscopy

Numerous methods exist for altering the size of pores distribution in a xerogel. The most straightforward variable to adjust for reducing pore width is the heat-treatment temp (or duration) [12, 13]. FT-IR spectroscopy offers comprehensive insights into the structural, chemical, and vibrational characteristics of many materials [14]. It was specifically utilized in the sol–gel-materials' characteriza-

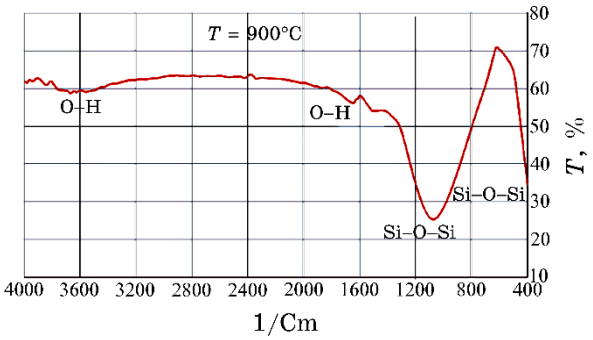

Fig. 2. FT-IR spectrum of undoped sol–gel xerogel of silica at 900°C.

tion, resulting in a comprehensive understanding of the correlation between molecular-level structure, IR spectra, and characteristics. Figure 2 illustrates the non-doped xerogel-of-silica specimen infrared-transmission spectrum, generated under synthetic conditions of pH 7 and a temperature of 900°C.

The band absorption at 460.2 cm^{-1} corresponds to the bend vibration of Si–O–Si sets; the peak at 810.1 cm^{-1} was related to the symmetrical stretch of Si–O–Si sets, and the wide band about 1103.8 cm^{-1} signifies the asymmetrical vibrations of Si–O–Si stretch [15, 16]. The subtle band at 964.8 cm^{-1}, ascribed to the vibrations of silanol stretch Si–OH sets, indicates a limited availability of these entities inside the silica network, suggesting that the condensation process was almost complete. The drying process at 110°C fails to eliminate water molecules inside the xerogel-of-silica pores, leading to the formation of two absorption bands. The first peak appears at 1640.7 cm^{-1} [16], corresponding to the bend vibrations of the oxygen–hydrogen bonding in water molecules, whereas the next peak at 3440 cm^{-1} is associated with the stretch vibration of the same bond [17]. Nonetheless, the intensity of the 1st band markedly decreased, and the 2nd band disappeared for the pure glass specimen sintering at 500°C, indicating that the bulk of H_2O molecules are eliminated throughout the sintering process.

3.2. Absorption Spectroscopy Measurements

This work utilized the UV–Visible spectrophotometer model (UV-6100PC) from EMC-LAB to get the spectrum of absorption of doped and non-doped xerogel of silica. Figures 3 and 4 show the spectra of optical absorption of Ce-doped and undoped xerogel of silica gained in an argon environment. The coefficient of absorption (α) in cm^{-1} is a wavelength (λ) function in nanometers [14].

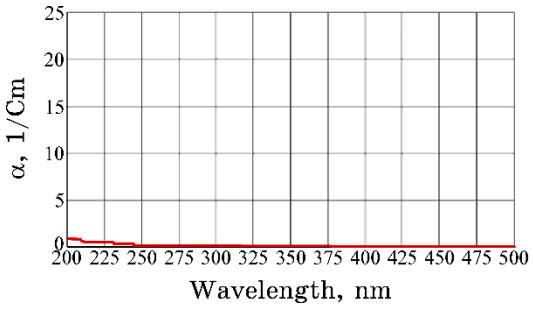

Fig. 3. Optical absorption spectrum of undoped xerogel of silica SiO_2Ar.

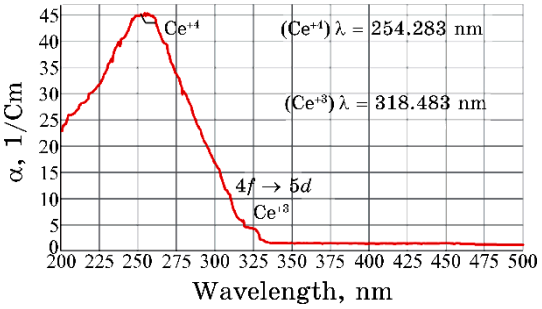

Fig. 4. Optical absorption spectrum of Ce-doped xerogel of silica SiO_2CeAr.

Figure 4 demonstrates that the SiO_2CeAr xerogel displays two absorption bands for each concentration in sample. The first band is centred at 254.283 nm ($E = 1240/254.283 = 4.87$ eV), whereas the subsequent band is at 318.483 nm (3.89 eV), attributed to Ce^{+4} ions and the $4f \rightarrow 5d$ transition of Ce^{+3} ions, respectively [14]. Furthermore, it has been utilized these spectra to ascertain the quantities of Ce ions and the associated cross-section absorption in both specimens. Initially, the maximum absorbance of Ce^{+4} in the SiO_2CeAr specimen was determined to be of $244.14 \cdot 10^{-23}$ cm^2; the amount of Ce^{+4} was inferred utilizing the previously established cross-section for Ce^{+4}.

Additionally, the amount of Ce^{+3} was computed, utilizing the maximum absorbance of Ce^{+3}; cross-section absorption (σ) of about $28.760 \cdot 10^{-23}$ cm^2 was found. Consequently, the derived ratio $\sigma(Ce^{+4})/\sigma(Ce^{+3})$ is of around 8.5. The proportions of 8.5 and the measured cross-section absorption are comparable to those reported for a Ce-doped xerogel of silica synthesized utilizing plasma torch chemical vapour deposition [18]. Conversely, decreased magnitude of the cross-section proportion was gained for Ce-activated alkali-silicate glasses [19].

3.3. Fluorescence Spectroscopy Measurements

This research assessed the fluorescence spectrum at ambient temperature utilizing a fluorescence spectrometer to get the emission spectra of both doped and non-doped xerogel of silica.

Figure 5 illustrates the light emission spectra of Ce-doped xerogel of silica gained in an argon environment. The intensity in arbitrary units is expressed as a function of wavelength (λ) expressed in nanometers.

Figure 5 displays the optical photoluminescence (PL) spectra of SiO_2CeAr gained under excitation at a wavelength of 365 nm, corresponding to energy of 3.39 eV ($E = 1240/365$ nm). The emitted luminescence is characterized by a wide band peaking at 456 nm (2.72 eV), having a full width at half max (FWHM) of 96 nm. This band is attributed to the permitted $5d \rightarrow 4f$ optical transition of Ce^{+3} ions [18, 20].

It is noteworthy that only the specimen subjected to inert circumstances exhibits a photoluminescence excitation spectrum associated with visible emission, characterized by a reasonably wide excitation band spanning from 254.283 to 456 nm and demonstrating good optical efficacy.

The spectral properties of the specimen resemble those of the glass. Its absorption spectrum clearly displays bands at 254.283 nm and 318.483 nm, corresponding to Ce^{+3} and Ce^{+4} ions, respectively. Furthermore, under 351 nm excitation, the luminescence at ambient temperature is primarily characterized by a visible emission at about 456 nm (3.06 eV), with a FWHM of 96 nm, due to Ce^{+3} ions. The covalence of the Ce–O bond rises, hence reducing the energy gap between the ground and excited states. To comprehend fully the cause of the detected red shift, more investigations into the alterations in the local structure of Ce^{+3} ions are necessary.

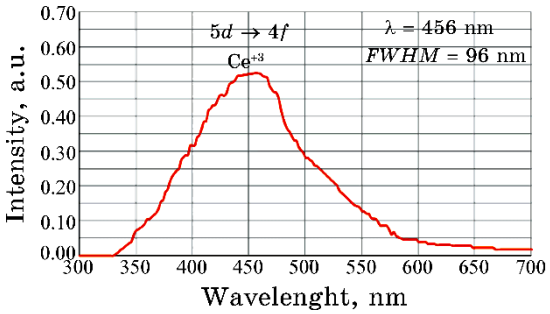

Fig. 5. Optical PL spectrum of SiO_2CeAr samples under the 365 nm excitation source.

3.4. Radioluminescent Spectroscopy Measurements

In the present work, it has been utilizing caesium isotopes have mass number 137 (Cs-137) and activity 7 mCi as a gamma rays' source for irradiation of sample at different doses 100, 200, 400, 500, and 2400 rad as shown in Table 2.

Figures 6 and 7 show the relationships of RL intensity and position as functions of gamma ray doses, respectively.

From the above results, it has been noticed the values of RL intensity increased with increasing of the gamma ray dose because increasing of the excitation state until the dose reaches 500 rad and

TABLE 2. Parameters for SiO_2CeAr sample with different doses of gamma rays.

D, rad	RL intensity, a.u.	λ, nm
100	0.557	456
200	0.592	458
400	0.619	460
500	0.64	462
2400	0.563	464

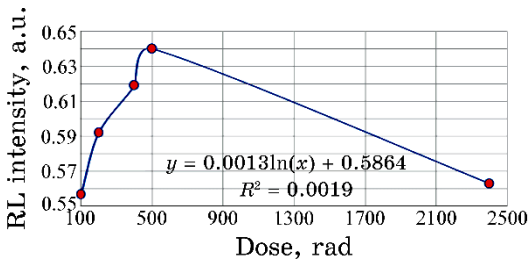

Fig. 6. RL intensity as a function of gamma ray doses.

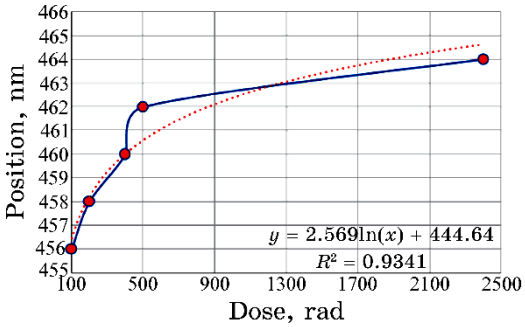

Fig. 7. Position as a function of gamma ray amount.

Fig. 8. Photograph of SiO_2CeAr xerogel of silica after irradiation with different gamma ray doses.

then started decreasing with increasing dose due to the ionic saturation, while the position of peaks of energy bands increased with increasing the gamma ray dose. Finally, the effect of irradiation of the samples has made them transparent as shown in Fig. 8.

4. CONCLUSIONS

The sol–gel process is a bottom-up synthesis method. In this process, the final products are formed by performing several irreversible chemical reactions. In this paper, studying the optical properties of silica xerogel doped with Ce for gamma ray detection, the selection of suitable catalysts, the operating mechanism of the catalysts, and the drying steps of the wet gel were investigated and different properties, Then, important applications of aerogels such as those in dosimeter for nuclear radiation, electronics and energy equipment, those as thermal and acoustic insulators, and those in catalysts, building materials, shock absorbers, and sensors were introduced.

Radiosensitive Ce-doped xerogel of silica has been synthesized with a low amount of doping *via* the sol–gel technique. The sol–gel materials exhibited an elevated Ce^{+3}/Ce^{+4} atomic proportion once densified in argon gas, leading to enhanced significantly photoluminescence emitting quantum efficacy in the visible spectrum. The Ar-treated glass was effectively utilized as the initial material to fabricate a millimetre-sized rod suitable for dosimetry experiments. It has been investigated the RL signal from a Ce-doped rod subjected to a large dosage of γ-rays for the first time. The strength of the RL signal increases with higher gamma ray amount until it approaches 500 rad, indicating that this material is a viable choice for radiation dosimetry utilization in hostile environments, particularly, in all-fibre sensor configurations. Moreover, the enhanced optical effectiveness of these Ce-activated xerogels could be utilized in

several fields, such as scintillators detecting ionizing radiation, as wavelength or UV-absorbing filters' converters in lighting systems.

REFERENCES

1. Z. S. Al-Khafaji, S. S. Radhi, M. M. Mahdi, N. S. Radhi, and B. M. Mareai, *AIP Conf. Proc.*, **2839**, No. 1: 1 (2023); https://doi.org/10.1063/5.0170939
2. Z. S. Al-Khafaji and M. W. Falah, *J. Adv. Res. Dyn. Control. Syst.*, **12**, No. 1: 666 (2020); https://doi.org/10.5373/JARDCS/V12SP1/20201115
3. S. S. Radhi, Z. S. Al-khafaji, and M. W. Falah, *HSD*, **4**, No. 1: 42 (2022); https://doi.org/10.37868/hsd.v4i1.82
4. N. K. Chaudhury, R. Gupta, and S. Gulia, *Def. Sci. J.*, **57**, No. 3: 241 (2007); https://doi.org/10.14429/dsj.57.1765
5. Nabaa S. Radhi, Ahlam Hamid Jasim, Zainab S. Al-Khafaji, and Mayadah Falah, *Nanosistemi, Nanomateriali, Nanotehnologii*, **21**, Iss. 4: 769 (2023); https://doi.org/10.15407/nnn.21.04.769
6. Ali S. Hasan, Mohammed Jawad H. Kadhim, Ali Y. Layla, and Zainab Al-Khafaji, *Opt. Quantum. Electron.*, **56**, Article No. 1781 (2024); https://doi.org/10.1007/s11082-024-07621-y
7. B. R. Smith and L. A. DeWerd, *Fundamentals of Radiation Physics and Dosimetry* (Radiat. Ther. Dosim.–CRC Press: 2021).
8. A. Safrany, A. Miller, and A. Kovacs, *Guidelines for the Development, Validation and Routine Control of Industrial Radiation Processes* (IAEA: 2013).
9. Francis Berghmans, Alberto Fernandez Fernandez, Benoit Brichard, Frans Vos, Marc C. Decreton, Andrei I. Gusarov, Olivier Deparis, Patrice Megret, Michel Blondel, Serge Caron, and Andre Morin, *SPIE Proc.*, **3538**: 28 (1999); https://doi.org/10.1117/12.335757
10. H. El Hamzaoui, L. Courthéoux, V. N. Nguyen, E. Berrier, A. Favre, L. Bigot, M. Bouazaoui, and B. Capoen, *Mater. Chem. Phys.*, **121**, Nos. 1–2: 83 (2010); https://doi.org/10.1016/j.matchemphys.2009.12.043
11. H. El Hamzaoui, G. Bouwmans, B. Capoen, Y. Ouerdane, G. Chadeyron, R. Mahiou, S. Girard, A. Boukenter, and M. Bouazaoui, *Mater. Res. Express.*, **1**, No. 2: 26203 (2014); https://doi.org/10.1088/2053-1591/1/2/026203
12. Yao Xi, Zhang Liangying, and Wang Sasa, *Sensors Actuators B Chem.*, **25**, Iss. 1–3: 347 (1995); https://doi.org/10.1016/0925-4005(95)85078-3
13. Carole C. Perry and Xiaochun Li, *J. Chem. Soc., Faraday Trans.*, **87**, Iss. 5: 761 (1991); https://doi.org/10.1039/ft9918700761
14. B. C. Smith, *Fundamentals of Fourier Transform Infrared Spectroscopy* (CRC Press: 2011).
15. Dimitris Davazoglou and Vassilis Em. Vamvakas, *JES.*, **150**, No. 5: F90 (2003); https://doi.org/10.1149/1.1562601
16. L. Yang, *Fabrication and Characterization of Microlasers by the Sol–Gel Method* (Dissertation (Ph.D.) (California Institute of Technology: 2005); doi:10.7907/HHQ8-VC25
17. Carla Cannas, Mariano Casu, Roberta Licheri, Anna Musinu, Giorgio Piccaluga, Adolfo Speghini, and Marco Bettinelli, *MRS Online Proc. Libr.*, **21**: Article No. 318 (2001); https://doi.org/10.1557/PROC-676-Y3.18

18. Yoshiro Ishii, Kazuo Arai, Hiroshi Namikawa, Mitsuhiro Tanaka, Akira Negishi, and Takashi Handa, *J. Am. Ceram. Soc.*, **70**, Iss. 2: 72 (1987); https://doi.org/10.1111/j.1151-2916.1987.tb04932.x
19. Marie-Laure Brandily-Anne, Julien Lumeau, Larissa Glebova, and Leonid B. Glebov, *J. Non. Cryst. Solids*, **356**, Iss. 44–49: 2337 (2010); https://doi.org/10.1016/j.jnoncrysol.2010.02.020
20. Carmen Canevali, Mariachiara Mattoni, Franca Morazzoni, Roberto Scotti, Mariano Casu, Anna Musinu, Radenka Krsmanovic, Stefano Polizzi, Adolfo Speghini, and Marco Bettinelli, *J. Am. Chem. Soc.*, **127**, Iss. 42: 14681 (2005); https://doi.org/10.1021/ja052502o